The face dependence of the effective electron mean free path derived from spherical-wave corrections in photoelectron diffraction of W(110) and W(100) surfaces

1989 J. Phys.: Condens. Matter 1 1879

(http://iopscience.iop.org/0953-8984/1/10/010)

J. Phys.: Condens. Matter 1 (1989) 1879–1888. Printed in the UK

The face dependence of the effective electron mean free path derived from spherical-wave corrections in photoelectron diffraction of W(110) and W(100) surfaces

G Tréglia†, M C Desjonquères‡, D Spanjaard†, D Sébilleau§, C Guillot‡§, D Chauveau‡§ and J Lecante‡§

† Laboratoire de Physique des Solides, Bâtiment 510, Université Paris-Sud, F91405 Orsay Cédex, France

‡ Service de Physique des Atomes et des Surfaces, CEN Saclay, F91191 Gif-sur-Yvette Cédex, France

§ Laboratoire d'Utilisation du Rayonnement Electromagnétique (CNRS–CEA–MEN), Batiment 209D, F91405 Orsay Cédex, France

Received 14 June 1988, in final form 12 September 1988

Abstract. We show that spherical-wave corrections can be of importance in a single-scattering calculation of the angular anisotropy of the photoemission from W(110) and W(100) 4f core levels. More precisely, for photon energies of about 65 eV, these corrections are sufficiently large to show the necessity, when using an isotropic electron mean free path λ_{ee}, to vary it according to the face under study. In our case, this leads to an effective electron mean free path λ_{ee} of 8 Å for W(110) and 5 Å for W(100). When this variation is allowed, the plane-wave approximation leads to results for W(110) which are in as good agreement with experiments as those for W(100). In particular, the influence of the hydrogen-induced reconstruction on the azimuthal patterns of W(110) is now very well reproduced.

1. Introduction

Owing to their increasing technological importance in problems such as corrosion or catalysis, metal surfaces have been the subject of a huge number of studies in the last decade. In the same time there has been considerable development of methods for determining the surface structure. Among them photoemission, and in particular core-level x-ray photoelectron spectroscopy, is a very sensitive probe of the chemical environment of the atom which undergoes excitation. More precisely, for kinetic energies of the outgoing electron in the range 20–200 eV, most of the signal originates from a few layers under the surface, owing to electron mean-free-path effects [1]. In this case, there exist several types of emitter (surface, first underlayer, ..., bulk atoms) with different geometrical environments, leading to core-level lines which should not appear strictly at the same energy. This is the so-called surface core-level shift which has given rise to many studies, especially in transition metals of the 5d series which present 4f lines sufficiently narrow to be separated experimentally (for reviews, see references [2–5]). Other interesting information which can be derived from core-level spectroscopy experiments is the variation in the intensity of the lines with the angle of observation and photon energy (i.e. photoelectron diffraction) which should be different for bulk and surface emissions. This has indeed been observed experimentally for the $4f_{7/2}$ core-level lines of W(100) [6] and W(110) [7] surfaces. Moreover, it has been shown in

0953-8984/89/101879 + 10 $02.50

these cases that a single-scattering plane-wave theory was sufficient to reproduce the experimental azimuthal patterns, perfectly for W(100) and qualitatively for W(110), even in the low-kinetic-energy range for which bulk and surface emissions are well separated [5, 7]. However, in this simple scheme, the question arises whether the assumption of replacing the spherical waves emerging from the emitting atom by plane waves around the scatterer is not too crude and what the influence of curved-wave corrections would be on these previous results. In particular, could these corrections improve the agreement between theory and experiments for W(110) [7]? The aim of this paper is to show that surprisingly, whereas they only slightly modify this agreement for W(100), they make it worse for W(110), at least for the value of the electron mean free path λ_{ee} (5 Å) used in our previous calculations. This is no longer true if we increase λ_{ee} (up to 8 Å) in which case both plane-wave and spherical-wave calculations now give similar azimuthal patterns, in much better agreement with experimental data for W(110). On the contrary, increasing λ_{ee} leads to poorer agreement for W(100). These somewhat contradictory results could be attributed to a face dependence of the isotropic effective electron mean free path used in the calculations.

2. Single-scattering treatment of photoelectron diffraction

The aim of surface photoelectron diffraction is to extract information on the surface atomic structure from the analysis of the angular variation in the intensity of the core lines. More precisely, the modulation of the photocurrent due to interference between the direct and scattered beams of electrons propagating towards the analyser is studied as a function of the photon energy $h\nu$ and emergence angles (polar angle ϑ and azimuthal angle φ). The resulting angular anisotropy should then differ for the emissions of surface and bulk atoms, owing to their different environments. In the single-scattering approximation, the intensity of the photocurrent for an arbitrary initial state l_i is written [5, 6, 8, 9]

$$I \propto \sum_{m_i=-l_i}^{m_i=l_i} k \left| \sum_{l,m} M_{lm,l_im_i} \left[Y_{lm}(\hat{\boldsymbol{R}}) \exp\left(\frac{-L}{2\lambda_{ee}}\right) + \sum_j Y_{lm}(\hat{\boldsymbol{R}}_j) \frac{\exp[ikR_j(1-\cos\vartheta_j)]}{R_j} f_{lm}(\vartheta_j) W_j \exp\left(-\frac{L_j}{2\lambda_{ee}}\right) \right] \right|^2 \tag{1}$$

where k is the modulus of the wavevector, Y_{lm} are the spherical harmonics, the detector is located at $\boldsymbol{R}$, the neighbour j is at distance R_j from the emitter, ϑ_j ($=\cos^{-1}(\hat{\boldsymbol{R}} \cdot \hat{\boldsymbol{R}}_j)$) is the scattering angle and $f_{lm}(\vartheta_j)$ the scattering factor:

$$f_{lm}(\vartheta_j) = \frac{4\pi}{k} \sum_{l'm'} [\exp(i\delta^j_{l'}) \sin\delta^j_{l'}\, Y_{l'm'}(\hat{\boldsymbol{R}}) Y^*_{l'm'}(\hat{\boldsymbol{R}}_j)] C_{lml'm'}(\boldsymbol{k}, \boldsymbol{R}_j) \tag{2}$$

in which $\delta^j_{l'}$ is the phase shift due to scatterer j ($j = 0$ for an emitter) and

$$M_{lm,l_im_i} = (-1)^l \exp(i\delta^0_l) \sum_{m'=-1}^{m'=-1} Y^*_{lm'}(\hat{\boldsymbol{\varepsilon}}) G(l_im_i, 1m'|lm) \tilde{\rho}_k(l, l_i)$$
$$\tilde{\rho}_k(l, l_i) = \int \mathcal{R}_l(kr) R_{l_i}(r) r^3 \, dr \tag{3}$$

where $\mathcal{R}_l(kr)$ is the regular solution of the radial Schrödinger equation of the emitter

atom and $R_{l_i}(r)$ the radial part of the initial state. $\hat{\boldsymbol{\epsilon}}$ is the polarisation vector and

$$G(l_i m_i, 1m'|lm) = \int \mathrm{d}\Omega\, Y_{l_i m_i}(\hat{r}) Y^*_{1m'}(\hat{r}) Y^*_{lm}(\hat{r})$$

is the Gaunt coefficient which vanishes except for $l = l_i \pm 1$, which are then the only allowed transitions. The inelastic effects have been introduced as an isotropic attenuation of the electronic amplitude due to the finite electron mean free path λ_{ee} and the thermal vibrations via a Debye–Waller factor $W_j = \exp[-2k^2(1 - \cos\vartheta_j)]\,\langle u_j^2\rangle$ where $\langle u_j^2\rangle$ is the one-dimensional mean-square displacement of the jth atom with respect to the emitter [10], $L(L_j)$ is the distance from the emitter to the surface (via the jth scatterer). Finally,

$$C_{lm,l'm'}(\boldsymbol{k}, \boldsymbol{R}_j) = \sum_{l''m''} c_{l''}(kR_j) Y^*_{l''m''}(\hat{\boldsymbol{R}}_j) G(lm, l''m''|l'm') \Big/ \sum_{l''m''} Y^*_{l''m''}(\hat{\boldsymbol{R}}_j) G(lm, l''m''|l'm')$$

$$c_{l''}(kR_j) = \mathrm{i}^{l''+1} kR_j \exp(-\mathrm{i}kR_j)\, h^{(1)}_{l''}(kR_j) \tag{4}$$

where $h^{(1)}_{l''}(kR_j)$ is the spherical Hankel function of the first kind and the summation over l'' is restricted to

$$l' - l \leqslant l'' \leqslant l' + l \qquad l'' + l' \text{ even}. \tag{5}$$

This expression can be simplified greatly by assuming that the spherical waves emerging from the emitting atom can be replaced by plane waves around the scatterer, i.e. by assuming that kR_j is sufficiently large to allow use of the asymptotic limit of the Hankel function:

$$h^{(1)}_{l''}(kR_j) \xrightarrow[kR_j \to \infty]{} (-\mathrm{i})^{l''+1} (kR_j)^{-1} \exp(\mathrm{i}kR_j). \tag{6}$$

Then, according to (4), $c_{l''}(kR_j) \to 1$ and $C_{lm,l'm'}(\boldsymbol{k}, \boldsymbol{R}_j) \to 1$. Therefore one recovers the usual scattering factor in the plane-wave approximation:

$$f_{lm}(\vartheta_j) \to f(\vartheta_j) = \frac{4\pi}{k} \sum_{l'm'} \exp(\mathrm{i}\delta^j_{l'}) \sin\delta^j_{l'}\, Y_{l'm'}(\boldsymbol{R}) Y^*_{l'm'}(\hat{\boldsymbol{R}}_j). \tag{7}$$

It is obvious from the comparison between (2) + (4) and (7) that the plane-wave approximation saves a huge amount of computational time, especially for large values of l_i (and then of l). Actually, some intermediate approximations have been proposed [11] based on a development of $h^{(1)}_{l''}$, up to next order in kR_j:

$$c_{l''}(kR_j) \simeq \sqrt{1 + l''(l''+1)/2(kR_j)^2}\, \exp[\mathrm{i}\, l''(l''+1)/2kR_j]. \tag{8}$$

Unfortunately, the practical interest of this simplification is mainly appreciable for an s initial state ($l_i = 0, l = 1$) and the calculations are almost as tedious as with the exact expression for $l_i \geqslant 1$. This is probably the reason why, up to now, the effects of curved-wave corrections have been investigated for s initial states only [9, 12, 13]. Here, we shall make a study of these corrections for the 4f levels ($l_i = 3$) of W(110) and W(100) surfaces in order to compare first the azimuthal photodiffraction patterns calculated using spherical or plane waves around the scatterers and then both results with the experimental data existing for these systems.

3. Spherical-wave corrections in photoelectron diffraction of W(110) and (100) surfaces

In our previous work [4–7], we have shown that a plane-wave single-scattering treatment of photoelectron diffraction was sufficient to account for the $4f_{7/2}$ azimuthal patterns

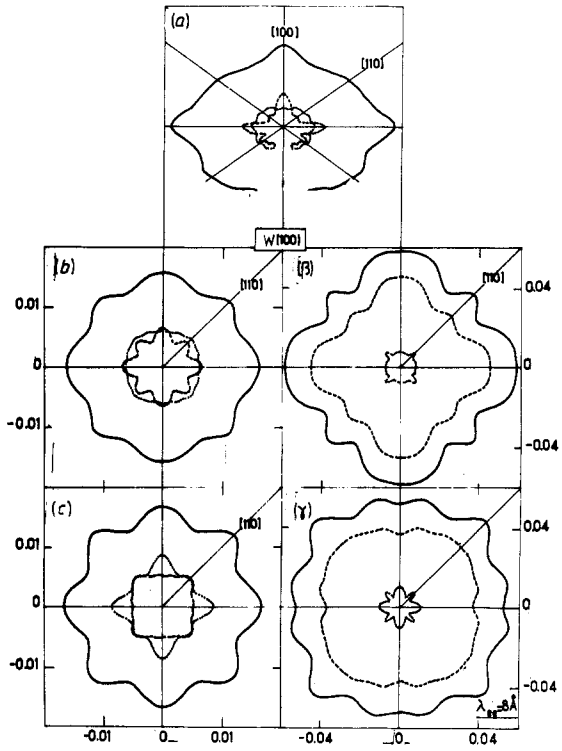

Figure 1. Polar plots of (*b*), (*c*), (*β*), (*γ*) the theoretical (single-scattering treatment including 'shadowing effects') and (*a*) the experimental azimuthal dependence of W(100) core photoelectron intensities for the total (——), bulk (– – –) and surface (. . .) emissions. The calculations have been performed for an f → d transition in (*b*), (*β*) the plane-wave and (*c*), (*γ*) the spherical-wave approximations for two values of the electron mean free path, (*b*), (*c*) $\lambda_{ee} = 5$ Å and (*β*), (*γ*) $\lambda_{ee} = 8$ Å, and for $\vartheta = 30°$, $\alpha = 22°5'$ and $h\nu = 65$ eV. (*a*) and (*b*) are taken from [5].

observed in the case of W(100) (compare figures 1(*a*) and 1(*b*)) and to a less extent W(110) (compare figures 2(*a*) and 2(*b*)), even in the low-kinetic-energy range ($E_c \simeq 30$ eV) for which bulk and surface emissions are well separated. Moreover, we have emphasised that it was important and sufficient to make the calculations for a transition from a realistic 4f ($l_i = 3$) initial state (and not from a simplified s state) towards the ($l = 2$) final state only (the transition $3 \rightarrow 4$ being negligible in view of the respective orders of magnitude of the radial matrix elements $\tilde{\rho}_k(4, 3)$ and $\tilde{\rho}_k(2, 3)$ at the energy of the experiments) [5, 6]. Then, if we also neglect here the transition $3 \rightarrow 4$, the radial matrix element factorises and (1) can be rewritten

$$I \propto \sum_{m_i=-3}^{m_i=3} \left| \sum_{m=-2}^{m=2} Y^*_{1,m-m_i}(\hat{\boldsymbol{\varepsilon}}) G(3m_i, 1(m-m_i)|2m) \left[Y_{2m}(\hat{\boldsymbol{R}}) \exp\left(-\frac{L}{2\lambda_{ee}}\right) + \sum_{j\neq 0} Y_{2m}(\hat{\boldsymbol{R}}_j) \frac{\exp[ikR_j(1-\cos\vartheta_j)]}{R_j} W_j \exp\left(-\frac{L_j}{2\lambda_{ee}}\right) f_{2m}(\vartheta_j) \right] \right|^2 . \quad (9)$$

In the plane-wave approximation previously used, the expression of the photocurrent was formally the same, the scattering factor $f_{2m}(\vartheta_j)$ being replaced by the simplified factor $f(\vartheta_j)$ (7). This led to the azimuthal patterns exhibited in figures 1(*b*) and 2(*b*) where we have plotted separately the total, bulk and surface emissions. Note that the emission from the first underlayer is not included in the bulk emission for W(100) whereas it is for W(110) since in the latter case the corresponding core-level line is not separated from the bulk line [2–5]. It is worth noting that these calculations [5, 6] took into account—somewhat inconsistently—the influence of some forward double-scattering events since, when two scatterers were aligned with the emitter, we eliminated

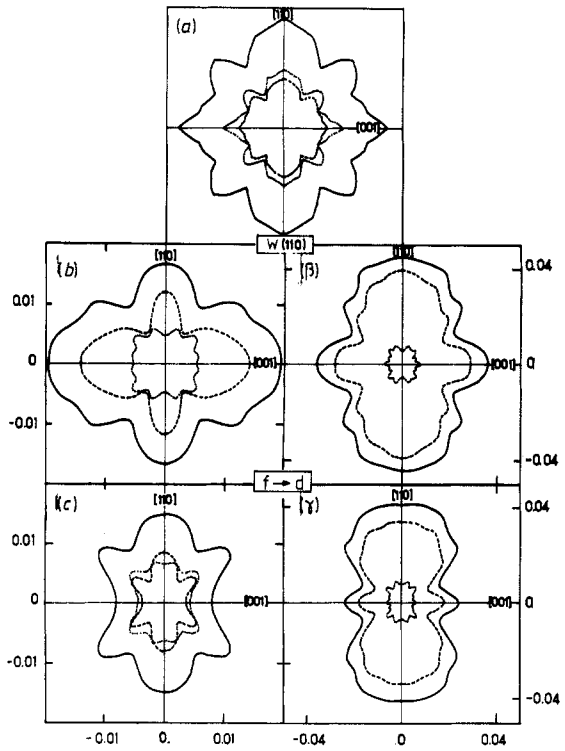

Figure 2. Polar plots of (*b*), (*c*), (*β*), (*γ*) the theoretical (single-scattering treatment including 'shadowing effects') and (*a*) the experimental azimuthal dependence of W(110) core photoelectron intensities for the total (——), bulk (– – –) and surface (. . .) emissions. The calculations have been performed for an f→d transition in (*b*), (*β*) the plane-wave and (*c*), (*γ*) the spherical-wave approximations for two values of the electron mean free path, (*b*), (*c*) $\lambda_{ee} = 5$ Å and (*β*), (*γ*) $\lambda_{ee} = 8$ Å, and for $\vartheta = 30°$, $\alpha = 22°5'$ and $h\nu = 65$ eV. (*b*) is taken from [5] and (*a*) derived from the results in [7].

the more distant one, thus introducing a kind of shadowing effect! Here, in order to perform a rigorous single-scattering treatment, we have reintroduced these scatterers which leads to patterns exhibited in figures 3(*b*) and 4(*b*). One sees that it does not affect the results for the (110) face whereas it induces some small changes for the (100) face. Nevertheless, our main result remains, namely that the agreement between theory and experiment is excellent for W(100) and satisfactory for W(110).

Let us now introduce the curve-wave corrections by replacing $f(\vartheta_j)$ (7) by $f_{2m}(\vartheta_j)$, exactly calculated from (2) + (4) for the first time. We have used the same experimental conditions as in our previous plane-wave calculations: polar angle ϑ of 30°; angle α between the polarisation vector $\hat{\boldsymbol{\epsilon}}$ and the surface normal of 22°5'; photon energy $h\nu$ of 65 eV.

The scattering factor has been derived from an APW relativistic potential [14], the summation being limited to four phase shifts (we have checked that it gives patterns which are indistinguishible from those obtained with 20 phase shifts) to make computer calculations feasible! The surface potential barrier between vacuum and bulk has been taken into account by allowing a slight refraction effect which changes the emergence angle ϑ of the photo-electron inside the solid to ϑ' ($\vartheta' = \sin^{-1}[(1 + V_0/E_k)\sin^2\vartheta]^{1/2}$ where $V_0 = -14$ eV is the inner potential and E_k the kinetic energy inside the metal) in vacuum. The isotropic electron mean free path at the energy of the experiment has been taken from [15]: $\lambda_{ee} = 5$ Å. Finally, the summation over j in (1) has been limited to scatterers for which $L_j \leqslant 1.6\lambda_{ee}$ (leading to clusters of about 30–40 atoms) and, consistently, the emission has been restricted to layers for which $L \leqslant 1.6\lambda_{ee}$ (third or fourth sublayer). The convergence of the calculation has been successfully checked by

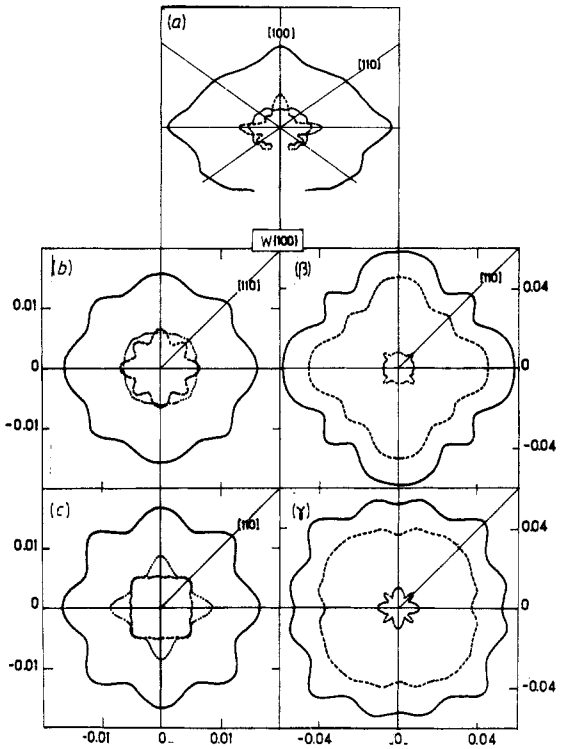

Figure 3. Same as figure 1 but for a rigorous single-scattering treatment. (*a*) is taken from [5].

extending the summation to scatterers for which $L_j \leqslant 2\lambda_{ee}$.

The resulting azimuthal patterns are shown in figures 3(*c*) and 4(*c*). Let us recall that they have been obtained from the exact spherical formulation, i.e. from (1) + (2) + (4). It is interesting to note that we have also used the intermediate approximation (8) [11] which leads to results completely indistinguishable from the previous results: the computer time being saved is negligible for $l_i = 3$. From the comparison between figures 3(*b*) and 3(*c*), 4(*b*) and 4(*c*), one sees at first glance that the curved-wave corrections modify only slightly the curves for W(100)—changing somewhat the bulk and surface emissions but not modifying the total emission—whereas they drastically change our results for W(110). In particular, the lobes pointing in the [001] directions are replaced by intensity minima in the latter case! Such a difference between the results of both approximations is very surprising, even at the low energies used here (for which kR_j is not so large, and then replacing $h_l(kR_j)$ by its asymptotic value is indeed not justified). For comparison, we have performed the same calculations for an s initial state. One can see in figure 5 that, in this case, curved-wave corrections induce only small modifications with respect to the plane-wave approximation for both surfaces (note that here also the plane-wave results slightly differ from those described in [4–6] owing to our complete neglect of 'shadowing effects' here). More surprisingly a comparison between figures 4(*b*) and 4(*c*) and figure 4(*a*) reveals that the results obtained in the plane-wave approximation for W(110) ($l_i = 3$) are in much better agreement with experiments than the more exact results including spherical corrections. This puzzling result implies that the qualitative agreement observed in [7] was somewhat fortuitous since improvements in the model tend to break it down. One should then wonder whether the single-scattering treatment itself is not oversimplified since, at low kinetic energies and for heavy atoms,

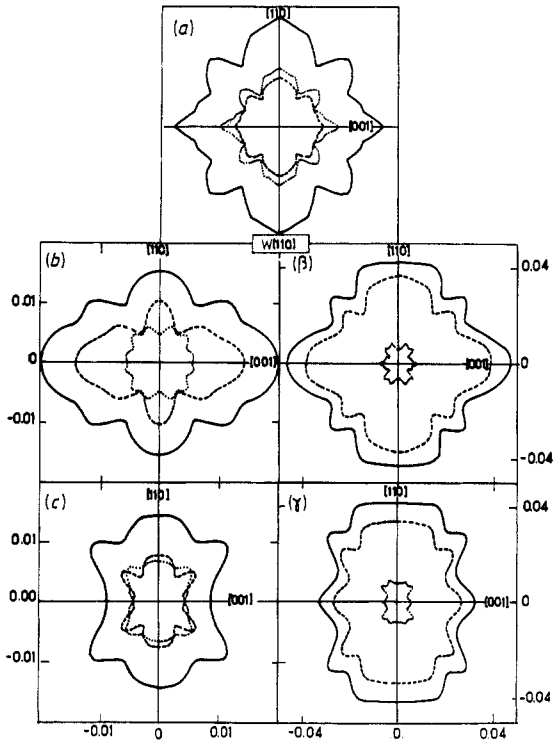

Figure 4. Same as figure 2 but for a rigorous single-scattering treatment. (*a*) is taken from the results in [7].

multiple-scattering (and possibly even relativistic scattering) effects are likely to prove important. However, taking into account these effects would lead to tedious calculations and the versatility of the single scattering would be lost. From this standpoint, it is tempting to check whether the precise value of some parameter in our problem could be more crucial in the improved calculation than in the approximate one. For instance, allowing small physical variations in the electron mean free path, which is a rather

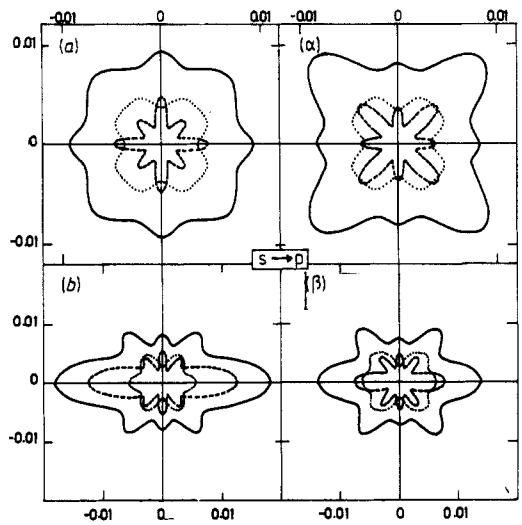

Figure 5. Polar plots of the theoretical (rigorous single-scattering treatment) azimuthal dependence of (*a*), (*α*) W(100) and (*b*), (*β*) W(110) core photoelectron intensities for the total (——), bulk (– – –) and surface (. . .) emissions. The calculations have been performed for an s → p transition in (*a*), (*b*) the plane-wave and (*α*), (*β*) the spherical-wave approximations for $\lambda_{ee} = 5$ Å, $\vartheta = 30°$, $\alpha = 22°5'$ and $h\nu = 65$ eV.

poorly known parameter, should modify the balance between distant and less distant neighbours for which the asymptotic form of the Hankel function is more or less justified. We shall see in § 4 that the spherical-wave calculation is indeed more sensitive to the precise value of λ_{ee} than is the plane-wave calculation, which will allow us to adjust it to the experimental data.

4. Role of the electron mean free path

A comparison of our value for λ_{ee} (5 Å) with those given in [1] for W (8 Å) seems to indicate that we have somewhat underestimated it. Therefore, it is tempting to use this larger value which, according to our above argument, should reinforce the contribution of distant neighbours for which the asymptotic value of $h_l^{(1)}$ is more justified and then improve the agreement between both calculations. This is indeed the case for W(110) as can be seen from figures 4(β) and 4(γ). The azimuthal patterns obtained by means of both approximations now exhibit the same structures in all directions, the plane-wave patterns being also perturbed but to a much less extent than the spherical-wave ones. Note that the difference in absolute intensities between bulk and surface emissions is much increased with respect to the calculation for $\lambda_{ee} = 5$ Å. This is due to the condition $L_{(j)} < 1.6\lambda_{ee}$ which implies that the bulk emission now contains emissions of layers up to the fifth sublayer (the corresponding average size of the scatterer clusters being of about 150 atoms). This can be compared with similar problems encountered in [16] during single-scattering plane-wave calculations for an overlayer of adsorbates on a given substrate. In that case the emission from the substrate was found to be too large compared with that of the adsorbate layer, the respective anisotropies being in satisfactory agreement, however, with experimental data. To avoid this discrepancy in [16] the scattering factor had to be reduced by an empirical damping factor (of about 2) which modified only the relative intensities of the two azimuthal patterns without changing the positions of the peaks. Here, being interested essentially in the separate azimuthal patterns, we shall not use this trick but shall keep in mind that one can empirically account for some effects which are not included in the theory (anisotropic inelastic scattering, multiple scattering and correlated vibrations for instance) by a damping of $f(\vartheta_j)$. Furthermore, if one compares figures 4(β) and 4(γ) with figure 4(a), one can see that now not only is the agreement between the results of both approximations improved but also so is the agreement between those calculations and the experimental data. This confirms that the crude agreement previously observed [7] ($\lambda_{ee} = 5$ Å; figure 4(b)) was indeed somewhat fortuitous. Thus, one can conclude from the comparison between the influence of curved-wave corrections on theoretical spectra and the experimental data for W(110)

(i) that the best value for an isotropic effective electron mean free path λ_{ee} should be 8 Å rather than 5 Å, and

(ii) that, for this value, one can use confidently the plane-wave approximation, the spherical-wave corrections being small.

Our results for W(100) are less clear since then increasing the value of λ_{ee} from 5 to 8 Å does not improve the agreement between both calculations nor between theory and experiments but instead tends to make it worse (see figures 3(β), 3(γ) and 3(a)). This is probably due to a competing effect between the increasing role of distant neighbours and the overestimation of the emission of deeper sublayers mentioned for W(110), which is more crucial here since, owing to the condition $L_{(j)} \leqslant 1.6\lambda_{ee}$, we now extend the bulk

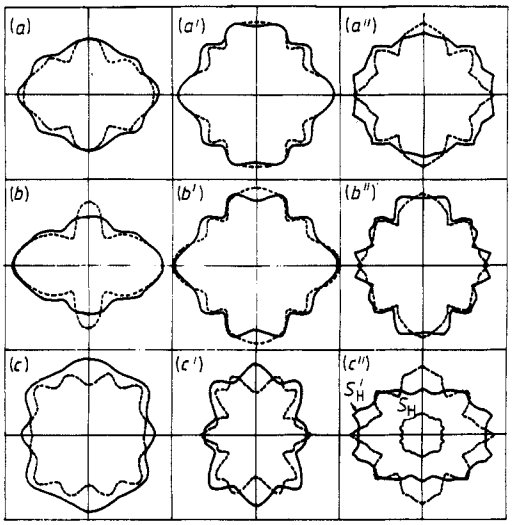

Figure 6. Influence of the hydrogen-induced reconstruction on the polar plots of the azimuthal dependence of W(110) core photoelectron intensities for (*a*), (*a'*), (*a''*) the total, (*b*), (*b'*), (*b''*) the bulk and (*c*), (*c'*), (*c''*) the surface emissions: ——, reconstructed surface; – – –, unreconstructed surface. The calculations have been performed for an f→d transition, in the plane-wave approximation, for two values of the electron mean free path: (*a*), (*b*), (*c*) λ_{ee} = 5 Å taken from [7] and (*a'*), (*b'*), (*c'*) λ_{ee} = 8 Å. (*a''*), (*b''*), (*c''*) The experimental data are taken from [7]. The experimental conditions are $\vartheta = 30°$, $\alpha = 22°5'$ and $h\nu$ = 65 eV.

emission up to the seventh sublayer. Then the omitted effect of anisotropic inelastic scattering should lead in that case to an empirical damping [16] of the scattering factor which is larger than for the (110) face. An alternative way of taking into account these anisotropic effects would be to allow a face dependence of the isotropic mean free path. In this respect, the value of λ_{ee} should in fact be 5 Å for the (100) face. However, let us remark that for this value, even though the agreement between calculations and experiments is now satisfactory, it remains poorer in the spherical-wave approximation for the separate bulk and surface emissions than for W(110) (λ_{ee} = 8 Å). The reason can perhaps be found now in some slight breakdown of the single-scattering approximation in that case. Let us recall that, in the plane-wave approximation, the influence of some of the main forward double-scattering events introduced some modifications in the bulk azimuthal patterns of W(100) (figures 1(*b*) and 3(*b*)) whereas no change could be seen for W(110) (figures 2(*b*) and 4(*b*)). The same conclusion holds in the presence of curved-wave corrections, namely the results are qualitatively unchanged for W(110) (compare figures 2(β) and 2(γ) with figures 4(β) and 4(γ)) whereas the agreement is improved for W(100) (compare figures 1(*b*), 1(*c*), 3(*b*) and 3(*c*) with figures 1(*a*) and 3(*a*)) when the 'shadowing effects' are taken into account.

5. Conclusion

In conclusion, we have shown that the curved-wave corrections to the 4f azimuthal photodiffraction patterns of W(110) and W(100) could be of importance in the low-energy range for which bulk and surface emissions are well separated. In particular, they are large enough to suggest an effective face dependence of the electron mean free path λ_{ee}, which is larger for the close-packed surfaces than for the open surfaces, to account for the experimental data in the framework of a single-scattering model. This 'effective' isotropic mean free path empirically accounts for effects which are not included in this theory: anisotropic inelastic scatterings, multiple scatterings and correlated vibrations which influence the relative importance of scatterers at different distances and in dif-

ferent geometries. Then, the plane-wave approximation can be used provided that one takes $\lambda_{ee} = 8$ Å for W(110) and $\lambda_{ee} = 5$ Å for W(100). As a consequence, our new results for W(110) are now in better agreement with experiments than our previous results were (with $\lambda_{ee} = 5$ Å) [7]. In this respect, it is tempting to re-examine the influence of hydrogen-induced reconstruction on W(110) azimuthal patterns [7] for $\lambda_{ee} = 8$ Å. Let us recall that, in presence of hydrogen, the (110) surface layer of W is rigidly displaced along the $\langle 1\bar{1}0 \rangle$ direction so that the surface atoms occupy threefold coordinated sites (rather than twofold ones) [17]. The results of the corresponding plane-wave calculations are compared in figure 6 with the previous calculations and with the experimental data. The agreement is greatly improved for the total and bulk emissions (the discrepancies for the surface emission coming from our neglect of hydrogen scatterers as already explained [7]) which defines the limits for using photodiffraction as a tool for determining the atomic structure of surfaces.

References

[1] Brundle C R 1974 *J. Vac. Sci. Technol.* **11** 212
[2] Guillot C 1985 *Thesis* Paris
[3] Spanjaard D, Guillot C, Desjonquères M C, Tréglia G and Lecante J 1985 *Surf. Sci. Rep.* **5** 1
[4] Desjonquères M C, Sébilleau D, Tréglia G, Spanjaard D, Guillot C, Chauveau D and Lecante J 1987 *Scanning Microsc.* **1** 1557
[5] Tréglia G, Sébilleau D, Desjonquères M C, Spanjaard D, Guillot C, Chauveau D and Lecante J 1988 *Springer Series in Solid State Sciences* vol 81 (Berlin: Springer) p 281
[6] Sébilleau D, Tréglia G, Desjonquères M C, Spanjaard D, Guillot C, Chauveau D and Lecante J 1988 *J. Physique* **49** 227
[7] Chauveau D, Guillot C, Villette B, Lecante J, Desjonquères M C, Sébilleau D, Spanjaard D and Tréglia G 1989 *Solid State Commun.* at press
[8] Fujikawa T 1981 *J. Phys. Soc. Japan* **50** 1321; 1982 *J. Phys. Soc. Japan* **51** 251; 1985 *J. Phys. Soc. Japan* **54** 2747
[9] Sagurton M, Bullock E L, Saiki R, Kaduwela A, Brundle C R, Fadley C S and Rehr J J 1986 *Phys. Rev.* B **33** 2207
[10] McDonnell L M, Woodruff D P and Holland B W 1975 *Surf. Sci.* **51** 249
[11] Rehr J J, Albers R C, Natoli C R and Stern E A 1986 *Phys. Rev.* B **34** 4350
[12] Rehr J J, Mustre de Leon J, Natoli C R and Fadley C S 1986 *J. Physique Coll.* **47** C8 213
[13] Barton J J and Shirley D A 1985 *Phys. Rev.* B **32** 1892
[14] Christensen N E and Feuerbacher B 1974 *Phys. Rev.* B **10** 2349
[15] Tokutaka H, Nishimori K and Hayashi H 1985 *Surf. Sci.* **149** 349
[16] Kono S, Goldberg S M, Hall N F T and Fadley C S 1980 *Phys. Rev.* B **22** 6085
[17] Chung J W, Ying S C and Estrup P J 1986 *Phys. Rev. Lett.* **56** 749